The American Journal of Pathology, Vol. 185, No. 4, April 2015

ELSEVIER

The American Journal of PATHOLOGY

ajp.amjpathol.org

TUMORIGENESIS AND NEOPLASTIC PROGRESSION

Activated Mutant p110α Causes Endometrial Carcinoma in the Setting of Biallelic *Pten* Deletion

Ayesha Joshi,* Christopher Miller, Jr,* Suzanne J. Baker,† and Lora H. Ellenson*

From the Department of Pathology and Laboratory Medicine, Weill Cornell Medical College, New York, New York; and the Department of Developmental Neurobiology,† St. Jude Children's Research Hospital, Memphis, Tennessee*

Accepted for publication December 3, 2014.

Address correspondence to Lora H. Ellenson, M.D., Weill Cornell University Medical College, 1300 York Avenue, Room F309D, New York, NY 10021. E-mail: lora.ellenson@med.cornell.edu.

PTEN and *PIK3CA* mutations occur with high frequency in uterine endometrioid carcinoma (UEC). Although *PTEN* mutations are present in complex atypical hyperplasia and carcinoma, *PIK3CA* mutations are restricted to carcinoma. We generated mouse models harboring *Pten* loss and/or activated *Pik3ca* in the endometrial epithelium to investigate their respective roles in the pathogenesis of UEC. Presence of an activated mutant *Pik3ca* on the background of *Pten* loss led to aggressive disease, with 100% of mice exhibiting carcinoma. Expression of *Pik3ca* with E545K mutation alone was unable to cause hyperplasia or cancer in the uterus and did not activate Akt as effectively as *Pten* deletion in short-term cultures of mouse endometrial epithelium, likely explaining the lack of phenotype *in vivo*. We also report that nuclear localization of FOXO1 correlated with *PTEN* mutational status irrespective of the *PIK3CA* status in endometrial cancer cell lines. Furthermore, gene expression profiles resulting from *Pten* loss or activation of *Pik3ca* in primary mouse endometrial epithelial cells exhibit minimal overlap. Thus, *Pten* and *Pik3ca* have distinct consequences on the activation of the phosphatidylinositol 3-kinase pathway in endometrial epithelium and are likely to affect other nonoverlapping cellular mechanisms involved in the development and progression of the most common type of uterine cancer. *(Am J Pathol 2015, 185: 1104–1113; http://dx.doi.org/10.1016/j.ajpath.2014.12.019)*

Endometrial carcinoma is a significant cause of morbidity and mortality worldwide, and in the United States, it is the eighth most common cause of cancer-related deaths in women.[1] Endometrial carcinoma is most often of endometrioid morphology, and is usually preceded by complex atypical hyperplasia (CAH). The development of both endometrial hyperplasia and uterine endometrioid carcinoma (UEC) is associated with unopposed estrogen stimulation and/or specific genetic alterations.[1] Approximately 30% to 80% of primary UECs harbor *PTEN* mutations,[2–4] with a similar frequency detected in CAH. In contrast, *PIK3CA* mutations occur in 20% to 40% of UECs and are rarely, if ever, found in CAH.

Phosphatase and tensin homolog (PTEN) and *PIK3CA* are main components of the phosphatidylinositol 3-kinase (PI3K)/AKT/PTEN pathway with opposing actions. *PIK3CA* encodes the p110α catalytic subunit of the PI3K complex and is considered an oncogene. As a component of PI3K, it is activated downstream of growth factor signaling, resulting in phosphorylation of phosphatidylinositol-4,5-phosphate (PIP2) to generate phosphatidlyinositol-3,4,5-phosphate (PIP3). PIP3 activates AKT, a protein kinase that regulates several downstream pathways that impinge on cell proliferation, cell growth, and apoptosis. In contrast, *PTEN* is a tumor-suppressor gene encoding a dual-specificity phosphatase, capable of dephosphorylating both proteins and lipids. Its most well-described activity is the conversion of PIP3 to PIP2, indirectly inhibiting the action of PI3K. Thus, by preventing AKT activation, PTEN inhibits cell proliferation.[5,6]

Most *PTEN* mutations in CAH and UEC are localized to exons encoding the lipid phosphatase domain, resulting in

Supported by NIH/National Cancer Institute grants RO1 CA188516 (S.J.B.) and R01 CA095427 (L.H.E).

Disclosures: None declared.

http://dx.doi.org/10.1016/j.ajpath.2014.12.019

loss of its ability to dephosphorylate PIP3.[2,7,8] *PIK3CA* mutations, E542K E545K (both in exon 9) and H1047R (in exon 20), are hotspots, found in endometrial carcinoma, as well as several other cancers and lead to constitutive activation of p110α.[5] Because loss of *PTEN* or activation of *PIK3CA* lead to activation of the pathway, it is reasonable to assume that they have similar downstream effects. However, as noted above, *PTEN* mutations are found in both CAH and UEC, whereas *PIK3CA* mutations are almost exclusively found in UEC, suggesting unique and nonoverlapping functions in endometrial carcinoma pathogenesis.

$Pten^{+/-}$ female mice develop CAH by 32 weeks of age, and at approximately 52 weeks of age, 25% of the $Pten^{+/-}$ female mice develop UEC. Both CAH and UEC exhibit complete loss of Pten expression, as a result of biallelic *Pten* inactivation by either loss of heterozygosity or intragenic mutations in the wild-type allele.[9,10] In this mouse model, the frequency of biallelic inactivation is similar in CAH and UEC, and we have previously shown that mismatch repair deficiency hastens inactivation of the remaining *Pten* allele and promotes the progression of hyperplastic lesions to UEC.[9] These observations suggest that, although biallelic inactivation of *Pten* is an early event in endometrial tumorigenesis, it may not be sufficient for progression to invasive carcinoma. Given the genetic analyses of primary human tumors, it seems likely that mutations in *PIK3CA* may promote progression to carcinoma.

To determine the effect of loss of *PTEN* and/or activated *PIK3C*A in the development of UEC, we have developed several genetic mouse models. The results reported herein demonstrate distinct roles of these two genes in the pathogenesis of endometrial carcinoma.

Materials and Methods

Animals

$Pten^{loxP/loxP}$ mice on a Balbc/129SvJ background and $Ksp1.3\text{-}Cre^{+/-}$ mice were obtained from The Jackson Laboratory (Bar Harbor, ME). To investigate the role of *Pik3ca*, a mouse line with a Cre-inducible mutant form of *Pik3ca* (designated as $Pik3ca^{E545K/+}$) was constructed in the laboratory of Dr. Suzanne Baker (St. Jude Children's Research Hospital, Memphis, TN). The $Pik3ca^{E545K/+}$ mouse contains a lox-STOP-lox cassette upstream of the *Pik3ca* gene containing the E545K mutation. In the presence of Cre, the stop codon is excised such that the mutant allele is expressed from its endogenous promoter. These mice were bred with $Pten^{loxP/loxP}$ strain to generate $Pten^{loxP/loxP}$;$Pik3ca^{E545K/+}$ ($Pten^{f/f}$;$Pik3ca^{E545K}$), $Pten^{loxP/loxP}$;$Pik3ca^{+/+}$ ($Pten^{f/f}$), $Pten^{+/+}$;$Pik3ca^{E545K/+}$ ($Pik3ca^{E545K}$), and $Pten^{loxP/+}$;$Pik3ca^{E545K/+}$ ($Pten^{f/+}$;$Pik3ca^{E545K}$) mice. Mice expressing Cre under the *Wnt7a* promoter ($Wnt7a\text{-}Cre^{+/-}$) were obtained from Dr. Kenneth S. Korach (National Institute of Environmental Health Science, Research Triangle Park, NC). $Pten^{f/f}$;$Pik3ca^{E545K}$ mice were crossed with the *Wnt7a-Cre* and *Ksp1.3-Cre* mice to generate the described genotypes. All animal experiments were performed in accordance with Institutional Animal Care and Use Committee guidelines.

IHC Staining

The uteri harvested from all mice at indicated time points were fixed in formalin and embedded in paraffin. Sections (5 μm thick) were processed for hematoxylin and eosin staining and immunohistochemical (IHC) analysis. For IHC, the slides were deparaffinized, rehydrated, and subjected to antigen retrieval by boiling in the microwave in 10 mmol/L sodium citrate. The Vectastain ABC reagent (Vector Labs, Burlingame, CA) was then used according to the manufacturer's protocol. Antibodies used were Pten (1:100), phospho-Akt S473 (1:100), β-catenin (1:800), p-Gsk3β (1:50), p-Pras40 (1:800), Stathmin (1:50), and FoxO1 (1:100), all from Cell Signaling Technologies (Beverly, MA). Two human tissue microarrays (TMAs), one containing 100 cases of normal cycling endometrium and the second with 96 cases of UEC (24 International Federation of Gynecology and Obstetrics grade 1, 37 International Federation of Gynecology and Obstetrics grade 2, and 35 International Federation of Gynecology and Obstetrics grade 3 cases) generated at Weill Cornell Medical College (New York, NY) under Institutional Review Board approval were also stained with FOXO1 antibody, as per the protocol described above.

Microdissection

Areas corresponding to CAH, UEC, or normal epithelium were microdissected from deparaffinized, rehydrated, hematoxylin-stained sections (5 μm thick) under light microscope visualization with a 26-gauge needle. The DNA was extracted using previously published protocols.[11,12]

Primary Uterine Epithelial Cell Cultures

Epithelial cells from uteri of $Pten^{f/f}$;$Pik3ca^{E545K}$, $Pten^{f/f}$, and $Pik3ca^{E545K}$ mice were prepared as described previously.[13] Briefly, the horns were slit lengthwise and digested in a solution containing 0.25% trypsin in Hanks' balanced salt solution for 1 hour at 4°C, followed by another incubation for 1 hour at 22°C. The tissue pieces were transferred to ice-cold Hanks' balanced salt solution and vortex mixed to release sheets of epithelial cells. The cell suspension was filtered through a 20 μm nylon mesh, and the epithelial sheets (retained on the filter) were collected and resuspended in Dulbecco's modified Eagle's medium/F12 (1:1), 10% charcoal-stripped fetal bovine serum, 20 mmol/L HEPES, 100 μg/mL streptomycin, 100 U/mL penicillin, and 2 mmol/L L-glutamine and insulin-transferrin-selenium supplement (1×). Cells were plated in 6-well dishes coated with 1:10 diluted Matrigel (Life Technologies, Grand Island, NY) and cultured at 37°C in an incubator with 5%

CO_2. After reaching 80% to 90% confluence, the cells were infected with adenoviruses expressing Cre or green fluorescent protein (GFP; control), as described previously,[13] for 48 hours. Cells were harvested for RNA or protein extraction. The RNA was used for RNA sequencing analysis and for subsequent validation of differentially expressed genes (DEGs) by real-time quantitative PCR (qPCR). Whole cell protein lysates were used for immunoblot analysis using Pten, phospho-Akt, and Akt antibodies (Cell Signaling Technologies), all at 1:1000 dilution. Actin antibody (Sigma, St. Louis, MO) was used for normalization.

Nuclear and Cytoplasmic Extract Preparation

Endometrial cancer cell lines Hec1A parental clone (Hec1A WT) and PTEN-deleted Hec1A (Hec1A clone 16) have been described previously.[14] KLE and RL95 cells were purchased from ATCC (Manassas, VA) and were cultured as per the ATCC protocol. Nuclear and cytoplasmic extracts were prepared using the NE-PER Nuclear Protein Extraction Kit from Thermo Fisher Scientific (Waltham, MA), as per the manufacturer's protocol. The extracts were resolved by 4% to 20% SDS-PAGE and transferred to a polyvinylidene difluoride membrane, and immunoblot analysis was performed using p-FOXO1 and FOXO1 antibodies. Lamin A/C and glyceraldehyde-3-phosphate dehydrogenase antibodies were used to ensure purity of the nuclear and cytoplasmic extracts, respectively. All antibodies were purchased from Cell Signaling Technologies and used at a dilution of 1:1000.

RNA Sequencing and Analysis

Total RNA was extracted from the cells using the RNeasy Plus Universal Micro kit (Qiagen, Valencia, CA), as per the manufacturer's instructions. After isolation, total RNA integrity was checked using a 2100 Bioanalyzer (Agilent Technologies, Santa Clara, CA), and samples with RNA integrity number value greater than eight were used for library preparation and sequencing. Library construction, template hybridization, and cluster amplification were performed using the TruSeq RNA Sample Preparation Kit version 2 (Illumina Inc., San Diego, CA). After cluster generation, sequencing by synthesis was performed on the HiSeq2000/1000 machine (Illumina Inc.).

The RNA sequencing data were analyzed using Genesifter software (Geospiza, Seattle, WA). Raw reads from an Illumina HiSeq2000 in fastq format were filtered to remove any reads that contained primarily adaptor/primer sequences. Reads were then aligned using Burrows-Wheeler Aligner against the genomic reference sequence for *Mus musculus* (Build 37.2). The *Mus musculus* (Build 37.2) reference sequence and annotation were pulled from RefSeq database (*http://www.ncbi.nlm.nih.gov/refseq*; last accessed November 12, 2014), and reads mapping to the genome were characterized as exon, intron, or intergenic (outside any annotated gene). These aligned data were then used to calculate gene expression by taking the total of exon and known splice reads for each annotated gene to generate a count value per gene. For each gene, a normalized expression value was generated in two ways: reads per mapped million (RPMM; which is calculated by taking the count value and dividing it by the number of million mapped reads) and RPMM per kilobase (RPMM value divided by the kilobase length of the longest transcript for each gene). The RPMM values were used for comparing gene expression across samples to remove the bias of different numbers of reads mapped per sample. RPMM per kilobase values were used for comparing relative expression of genes to one another to remove the bias of different numbers of mapped reads and different transcript lengths. Samples were initially analyzed in a pairwise fashion with normalization by the number of million mapped reads (not including rRNA, tRNA, snRNA, or mitochondrial RNA), followed by likelihood ratio test, and Benjamini and Hochberg correction testing for significance via Bioconductor. After the statistical qualification of expression values, the data were filtered for genes that were threefold differentially expressed. A multiple sample analysis was also performed wherein GFP-treated (control) cells were compared to Cre-treated cells from $Pten^{f/f}$;$Pik3ca^{E545K}$, $Pten^{f/f}$, and $Pik3ca^{E545K}$ genotypes. For this analysis, the data were filtered for genes that were also threefold differentially regulated, and a Kyoto Encyclopedia of Genes and Genomes pathway analysis was performed. We initially focused on genes in the endometrial cancer and Wnt signaling pathways.

qPCR Validation of DEGs

Validation of DEGs was done by qPCR. We first used cDNA prepared from the same RNA used for RNA sequencing as technical validation. For biological validation, RNA was extracted from adenovirus-Cre–treated primary cultures of epithelial cells from at least two independent experiments, as described in *Materials and Methods*. RNA (1.0 μg) was reverse transcribed using the High Capacity RNA-to-cDNA Kit (Life Technologies), as per the manufacturer's instructions. Volume of reverse transcriptase reaction corresponding to 25 ng cDNA was used to set up qPCRs using TaqMan primer-probe sets from Life Technologies in the StepOnePlus PCR machine, and fold differences in gene expression were calculated using the $-\Delta\Delta C_T$ method.

Results

$Pik3ca^{E545K/+}$ Mutation Causes Carcinoma in the Setting of Biallelic *Pten* Deletion

The epithelium-restricted expression levels of the *Wnt7a*[15] and *Ksp1.3*[16–18] promoters in the endometrium have been described previously. Therefore, $Pten^{f/f}$;$Pik3ca^{E545K}$ mice were crossed with two mouse strains expressing Cre under *Wnt7a* (*Wnt-Cre*) or *Ksp1.3* (*Ksp-Cre*) promoters to delete *Pten* or express mutant activated *Pik3ca* in the uterine epithelium.

Uteri of *Wnt-Cre*$^{+/-}$;*Pten*$^{f/+}$;*Pik3ca*^{E545K}, *Wnt-Cre*$^{+/-}$;*Pten*$^{f/+}$, and *Wnt-Cre*$^{+/-}$;*Pik3ca*^{E545K} mice were analyzed at 5 months of age. This time point was determined due to the development of lymphoma and breast cancers in many of the *Wnt-Cre*$^{+/-}$;*Pten*$^{f/+}$;*Pik3ca*^{E545K} mice at this age. The *Wnt-Cre* and *Pten*$^{f/f}$;*Pik3ca*^{E545K} crosses never produced *Wnt-Cre*$^{+/-}$;*Pten*$^{f/f}$;*Pik3ca*^{E545K} or *Wnt-Cre*$^{+/-}$;*Pten*$^{f/f}$ mice, likely due to embryonic expression of *Wnt7a* with subsequent lethality. Ten of 15 *Wnt7a-Cre*$^{+/-}$;*Pten*$^{f/+}$;*Pik3ca*^{E545K} and 12 of 17 *Wnt-Cre*$^{+/-}$;*Pten*$^{f/+}$ female mice developed CAH (Figure 1A and Table 1). Only two *Wnt-Cre*$^{+/-}$;*Pten*$^{f/+}$;*Pik3ca*^{E545K} mice exhibited *in situ* carcinoma and/or myoinvasive carcinoma. We did not observe significant differences between the number of CAH foci and severity of disease between *Wnt-Cre*$^{+/-}$;*Pten*$^{f/+}$ and *Wnt7a-Cre*$^{+/-}$;*Pten*$^{f/+}$;*Pik3ca*^{E545K} genotypes. Interestingly, uteri of *Wnt-Cre*$^{+/-}$;*Pten*$^{f/+}$;*Pik3ca*^{E545K} mice exhibited lymphatic dilation and hemorrhagic cysts (Figure 1B). Of 15 *Wnt7a-Cre*$^{+/-}$;*Pten*$^{f/+}$;*Pik3ca*^{E545K} mice, 9 also developed lymphoma and breast lesions, likely due to expression of *Wnt-Cre* in these tissues. None of the 17 *Wnt-Cre*$^{+/-}$;*Pten*$^{f/+}$ mice developed hemorrhagic cysts, lymphomas, or breast lesions. All *Wnt-Cre*$^{+/-}$;*Pik3ca*^{E545K} mice ($n = 7$) exhibited normal uterine histological features at 5 months of age and also lacked hemorrhagic cysts, lymphoma, and breast lesions.

Mating of *Pten*$^{f/f}$;*Pik3ca*^{E545K} and *Ksp1.3-Cre* mouse strains generated *Ksp-Cre*$^{+/-}$;*Pten*$^{f/+}$;*Pik3ca*^{E545K}, *Ksp-Cre*$^{+/-}$;*Pten*$^{f/+}$, *Ksp-Cre*$^{+/-}$;*Pten*$^{f/f}$, *Ksp-Cre*$^{+/-}$;*Pten*$^{f/f}$;*Pik3ca*^{E545K}, and *Ksp-Cre*$^{+/-}$;*Pik3ca*$^{E545K/+}$ genotypes. Previously published work from our laboratory demonstrated that *Pten*$^{f/f}$ mice injected with adeno-Cre virus developed carcinoma between 2 and 4 months after injection.[13] We, therefore, chose to sacrifice mice of the five genotypes mentioned above at 4 months of age (Table 2). Eleven of 12 *Ksp-Cre*$^{+/-}$;*Pten*$^{f/+}$;*Pik3ca*^{E545K} and 12 of 16 *Ksp-Cre*$^{+/-}$;*Pten*$^{f/+}$ mice exhibited CAH only. The number of foci of CAH was comparable in *Ksp-Cre*$^{+/-}$;*Pten*$^{f/+}$;*Pik3ca*^{E545K} and *Ksp-Cre*$^{+/-}$;*Pten*$^{f/+}$ genotypes, to those observed in the *Wnt7a-Cre*$^{+/-}$;*Pten*$^{f/+}$;*Pik3ca*^{E545K} mice and the *Wnt-Cre*$^{+/-}$;*Pten*$^{f/+}$ mice. However, in the *Wnt7a-Cre*$^{+/-}$;*Pten*$^{f/+}$;*Pik3ca*^{E545K} genotype, two mice developed invasive carcinomas that were not observed in the *Ksp-Cre*$^{+/-}$;*Pten*$^{f/+}$;*Pik3ca*^{E545K} mice. All *Ksp-Cre*$^{+/-}$;*Pten*$^{f/f}$ mice ($n = 8$) developed extensive endometrial disease, with CAH involving the entire luminal and glandular epithelium (Figure 1C). In five of eight mice, CAH exhibited squamous metaplasia (Figure 1D). Only one mouse (12%) showed carcinoma with myometrial invasion. Hematoxylin and eosin analysis of *Ksp-Cre*$^{+/-}$;*Pten*$^{f/f}$;*Pik3ca*^{E545K} uteri ($n = 6$) showed CAH with squamous metaplasia and carcinoma with myometrial invasion (Figure 1, E and F) in all of the mice. In five mice, the gross examination of the uterus demonstrated enlarged uteri with ovaries engulfed by cysts that could not be distinguished from the oviduct (Figure 1G) as compared to *Ksp-Cre*$^{+/-}$;*Pten*$^{f/f}$ mice (Figure 1H). The carcinoma was well to moderately differentiated and extended into and completely surrounded the

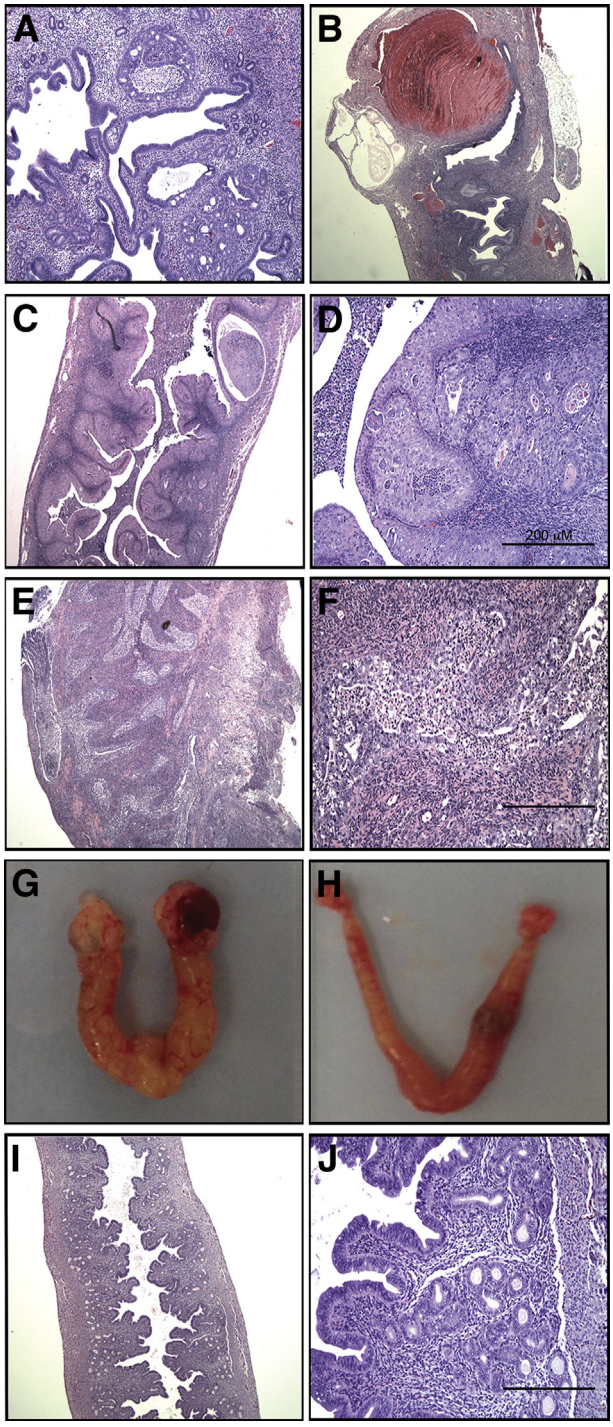

Figure 1 Photomicrographs of hematoxylin and eosin (H&E)—stained mouse uteri. **A** and **B:** Complex atypical hyperplasia (CAH; **A**) and hemorrhagic cysts (**B**) in *Wnt-Cre*$^{+/-}$;*Pten*$^{f/+}$;*Pik3ca*^{E545K} uteri at 5 months of age. **C:** Low-magnification H&E image of *Ksp-Cre*$^{+/-}$;*Pten*$^{f/f}$ mice with CAH involving entire luminal and glandular epithelium. **D:** High-magnification image of CAH with areas of squamous metaplasia. **E** and **F:** Low-magnification (**E**) and high-magnification (**F**) image of *Ksp-Cre*$^{+/-}$;*Pten*$^{f/f}$;*Pik3ca*^{E545K} uteri with carcinoma and myometrial invasion. **G:** Gross morphological features of *Ksp-Cre*$^{+/-}$;*Pten*$^{f/f}$;*Pik3ca*^{E545K} uteri with both ovaries engulfed in cysts. **H:** Gross morphological features of *Ksp-Cre*$^{+/-}$;*Pten*$^{f/f}$ mice exhibiting uterine disease but normal ovaries. **I:** Low-magnification H&E image of *Ksp-Cre*$^{+/-}$;*Pik3ca*^{E545K} uterus with normal histological features. **J:** High-magnification image of **I**. Original magnifications: ×200 (**A**, **D**, **F**, and **J**); ×40 (**B**, **C**, **E**, and **I**).

Table 1 Endometrial Lesions in *Wnt-Cre*$^{+/-}$;*Pten*$^{f/+}$;*Pik3ca*^{E545K} Mice and Littermates

Genotype	No. of mice	Mice with endometrial pathological features	Mice with CAH	Average No. of CAH foci	Mice with CA/Inv	Breast/lymph node pathological features
Wnt-Cre$^{+/-}$;*Pten*$^{f/+}$;*Pik3ca*^{E545K}	15	10	8	6–7	2	9
Wnt-Cre$^{+/-}$;*Pten*$^{f/+}$	17	12	12	7–8	0	0
Wnt-Cre$^{+/-}$;*Pik3ca*^{E545K}	7	0	0	0	0	0

CA, carcinoma; CAH, complex atypical hyperplasia; Inv, invasion.

ovaries (Figure 1G). Thus, the presence of a mutant *Pik3ca* on the background of biallelic *Pten* deletion resulted in extensive invasive carcinoma with 100% penetrance. None of the *Ksp-Cre*$^{+/-}$;*Pik3ca*^{E545K} mice developed endometrial disease (Figure 1, I and J), similar to *Wnt-Cre*$^{+/-}$;*Pik3ca*^{E545K} mice.

Expression of *Pik3ca*^{E545K} Does Not Cause Endometrial Carcinoma and Is Less Efficient at Activating Akt in Epithelial Cells

Carcinoma and/or CAH did not develop in mice regardless of the promoter used to activate *Pik3ca*. This lack of phenotype could be due to inefficient DNA recombination of the mutant *Pik3ca* allele or lack of clonal selection in endometrial epithelial cells expressing mutant *Pik3ca*. To determine the reason, we used PCR analysis to ascertain excision of the STOP codon upstream of exon 1 in the *Pik3ca* mutant allele by Cre recombinase. Presence of a recombined allele leads to amplification of a 735-bp band, whereas the nonrecombined allele amplifies a 637-bp band. Areas of CAH and carcinoma were microdissected from tissue sections of *Ksp-Cre*$^{+/-}$;*Pten*$^{f/f}$;*Pik3ca*^{E545K}, *Ksp-Cre*$^{+/-}$;*Pten*$^{f/f}$, and *Ksp-Cre*$^{+/-}$;*Pten*$^{f/+}$;*Pik3ca*^{E545K} uteri. DNA was extracted and analyzed by PCR. DNA from *Ksp-Cre*$^{+/-}$;*Pten*$^{f/f}$;*Pik3ca*^{E545K} and *Ksp-Cre*$^{+/-}$;*Pten*$^{f/+}$;*Pik3ca*^{E545K} uteri amplified both 637- and 735-bp bands (Figure 2A), proving that the mutant allele had undergone recombination in the lesions from these mice. DNA extracted from *Ksp-Cre*$^{+/-}$;*Pten*$^{f/f}$ uteri amplified only a 637-bp band, as expected (Figure 2A). DNA was also extracted from normal epithelium of *Ksp-Cre*$^{+/-}$;*Pik3ca*^{E545K} mice and PCR amplified a 637-bp nonrecombined band, but a faint 735-bp band from the recombined allele was detected (Figure 2A). This observation suggested that even though recombination occurred, epithelial cells with the recombined allele do not have a significant growth advantage in this setting.

We also performed IHC analysis on the tissue sections using p-Akt antibody. Although areas of CAH and carcinoma in all of the genotypes with endometrial pathological features (Figure 2B) exhibited characteristic membrane staining for p-Akt, the epithelium or glands in *Ksp-Cre*$^{+/-}$;*Pik3ca*^{E545K} mice (Figure 2C) were completely negative for p-Akt. The uteri of *Wnt-Cre*$^{+/-}$;*Pik3ca*^{E545K} mice were also negative for p-Akt staining (data not shown).

Pik3ca was activated *in vitro* by adeno-Cre treatment of primary epithelial cells isolated from *Pten*$^{f/f}$ and *Pten*$^{f/f}$;*Pik3ca*^{E545K} mice. Adeno-GFP–treated cells were used as control cells (GFP). We have previously demonstrated that *in vitro* adeno-Cre–mediated *Pten* deletion in epithelial cells results in activation of Akt.[13] In cells prepared from *Pik3ca*^{E545K} mice, Akt was activated but was severalfold lower than that observed in *Pten*$^{f/f}$ or *Pten*$^{f/f}$;*Pik3ca*^{E545K} cells (Figure 2D). Thus, mutant *Pik3ca* alone results in a much less robust activation of Akt, compared to loss of Pten, in endometrial epithelial cells. Quantitation of the immunoblot analysis is depicted in Figure 2E.

Expression of Downstream Signaling Molecules in the PI3K/Pten/Akt Pathway

Next, we performed IHC analysis on uterine sections from *Ksp-Cre*$^{+/-}$;*Pten*$^{f/+}$, *Ksp-Cre*$^{+/-}$;*Pten*$^{f/+}$;*Pik3ca*^{E545K}, *Ksp-Cre*$^{+/-}$;*Pten*$^{f/f}$, and *Ksp-Cre*$^{+/-}$;*Pten*$^{f/f}$;*Pik3ca*^{E545K} mice with antibodies against p-Gsk3β, p-Pras40, Stathmin, and FoxO1, which are known substrates of p-Akt. IHC analysis was also performed using antibodies against β-catenin because cytoplasmic and nuclear accumulation of β-catenin has been associated with squamous metaplasia. In the genotypes with CAH and carcinoma, the lesions expressed p-Gsk3β and p-Pras40 (Figure 3, A and B), whereas normal epithelium was negative (Figure 3, A and B), correlating with activation of the pathway. Stathmin and β-catenin

Table 2 Endometrial Lesions in *Ksp-Cre*$^{+/-}$;*Pten*$^{f/f}$;*Pik3ca*^{E545K} Mice and Littermates

Genotype	No. of mice	Mice with endometrial pathological features	Mice with CAH	Average No. of CAH foci	Mice with CA/Inv
Ksp-Cre$^{+/-}$;*Pten*$^{f/+}$;*Pik3ca*^{E545K}	12	11	11	8	0
Ksp-Cre$^{+/-}$;*Pten*$^{f/+}$	16	12	12	9–10	0
Ksp-Cre$^{+/-}$;*Pik3ca*^{E545K}	6	0	0	0	0
Ksp-Cre$^{+/-}$;*Pten*$^{f/f}$	8	8	8	Extensive	1
Ksp-Cre$^{+/-}$;*Pten*$^{f/f}$;*Pik3ca*^{E545K}	6	6	6	Extensive	6

CA, carcinoma; CAH, complex atypical hyperplasia; Inv, invasion.

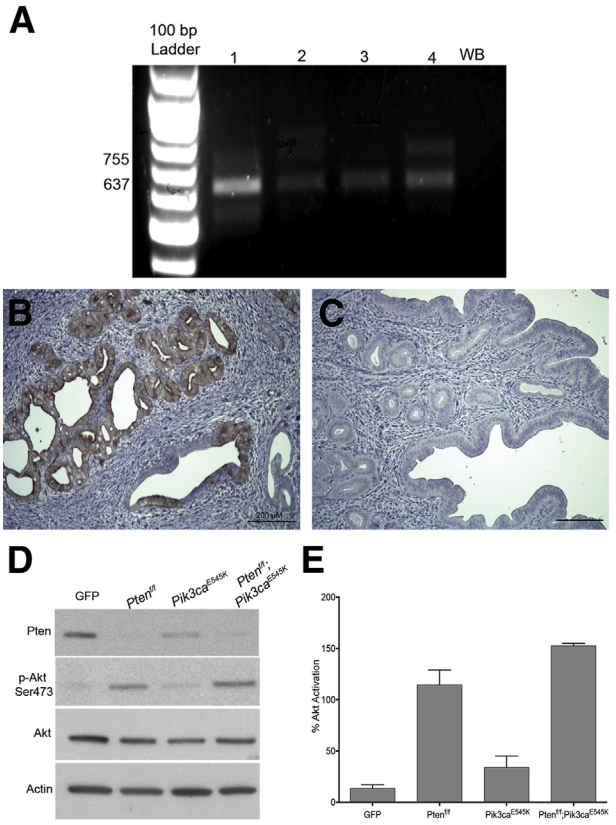

Figure 2 Recombination of mutant *Pik3ca* allele and activation of Akt in primary cultures. **A:** Agarose gel electrophoresis of PCR analysis of DNA extracted from microdissected, formalin-fixed, paraffin-embedded tissue from *Ksp-Cre*$^{+/-}$;*Pik3ca*^{E545K} (lane 1), *Ksp-Cre*$^{+/-}$;*Pten*$^{f/+}$;*Pik3ca*^{E545K} (lane 2), *Ksp-Cre*$^{+/-}$;*Pten*$^{f/f}$ (lane 3), and *Ksp-Cre*$^{+/-}$;*Pten*$^{f/f}$;*Pik3ca*^{E545K} (lane 4) mice. **B** and **C:** p-Akt immunohistochemical analysis of uterine sections of *Ksp-Cre*$^{+/-}$;*Pten*$^{f/+}$;*Pik3ca*^{E545K} (**B**) and *Ksp-Cre*$^{+/-}$;*Pik3ca*^{E545K} (**C**) mice. **D:** Immunoblot analysis of whole cell extracts of Adeno-GFP or Adeno-Cre–treated primary uterine epithelial cells isolated from *Pten*$^{f/f}$, *Pik3ca*^{E545K}, and *Pten*$^{f/f}$;*Pik3ca*^{E545K} mice using Pten, p-Akt, Akt, and actin antibodies. **E:** Quantitation of p-Akt in **D**. Graph represents p-Akt/Akt ratios from three independent experiments. Data represent means ± SD. GFP, green fluorescent protein; WB, water blank.

expression was not altered, and β-catenin was localized to cell membranes in normal and neoplastic cells, even in areas of squamous metaplasia (Supplemental Figure S1). FoxO1 expression was also significantly altered. FoxO1 localization was nuclear in normal epithelium and stromal cells (Figure 3C), but areas of CAH (Figure 3C) and carcinoma (Figure 3D) exhibited complete lack of nuclear FoxO1 with reduced cytoplasmic expression, irrespective of the genotypes. Pras40, Gsk3β, and FoxO1, therefore, are likely downstream targets of Pten inactivation in the uterine epithelium. IHC analysis with FOXO1 antibody was also performed on TMAs of human endometrial carcinomas and normal cycling (proliferative and secretory) endometria. Intense nuclear expression was observed only in the normal secretory epithelium but was absent in normal proliferative epithelium, as reported previously.[19] In contrast, 72% of carcinomas (69 of 96 cases) lacked nuclear FOXO1 expression. More important, the results with the human TMA (Supplemental Table S1) corroborate the results found in our genetic mouse model.

To further investigate lack of nuclear FOXO1, we analyzed several endometrial cancer cell lines for subcellular distribution and phosphorylation status of FOXO1 by immunoblot analysis. Nuclear and cytoplasmic extracts were prepared from KLE, RL95, Hec1A WT, and Hec1A clone16 (isogenic clone with somatic deletion of *PTEN*) cell lines with unique combinations of mutations (Supplemental Table S2) in *PTEN* and *PIK3CA*. FOXO1 was detected in both the cytoplasm and the nucleus in Hec1A WT and KLE cells (Figure 3E). In contrast, the Hec1A clone 16 and RL95 (mutated for *PTEN*) cell lines lacked nuclear FOXO1 expression and demonstrated reduced cytoplasmic expression. This observation correlates with the mouse studies

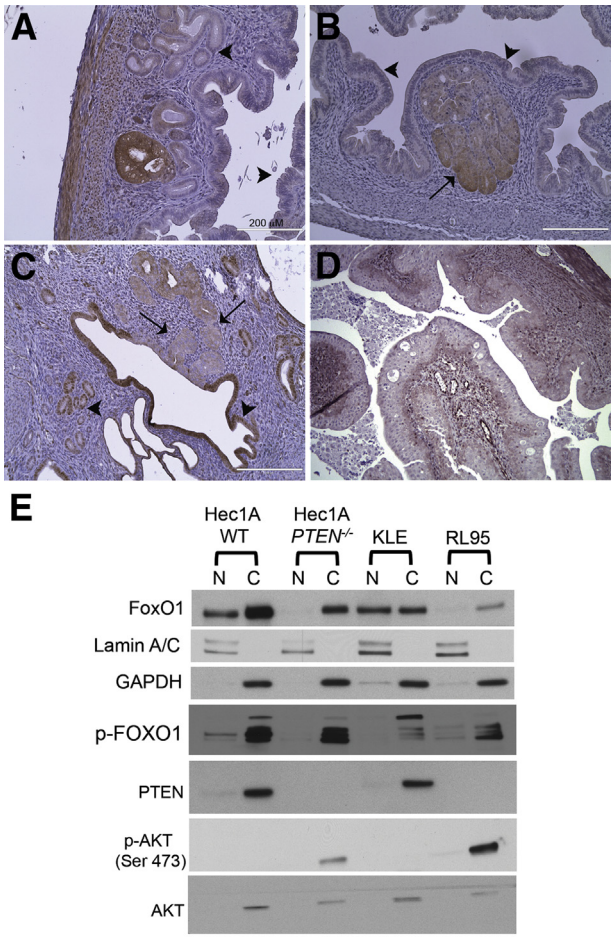

Figure 3 Immunohistochemical (IHC) analysis of downstream signaling molecules. **A** and **B:** Positive IHC staining with p-Gsk3β (**A**) and p-Pras40 (**B**) antibodies in uteri with complex atypical hyperplasia (CAH; **arrow**) as compared to normal epithelium (**arrowheads**). **C:** Loss of nuclear FoxO1 staining in CAH (**arrows**) compared to the intense nuclear staining of normal epithelium (**arrowheads**). **D:** Loss of nuclear FoxO1 in carcinoma. **E:** Immunoblot analysis depicting subcellular localization of FOXO1 in endometrial cancer cell lines. Lamin A/C and glyceraldehyde-3-phosphate dehydrogenase (GAPDH) served as controls to determine relative purity of nuclear (N) and cytoplasmic (C) extracts. WT, wild type.

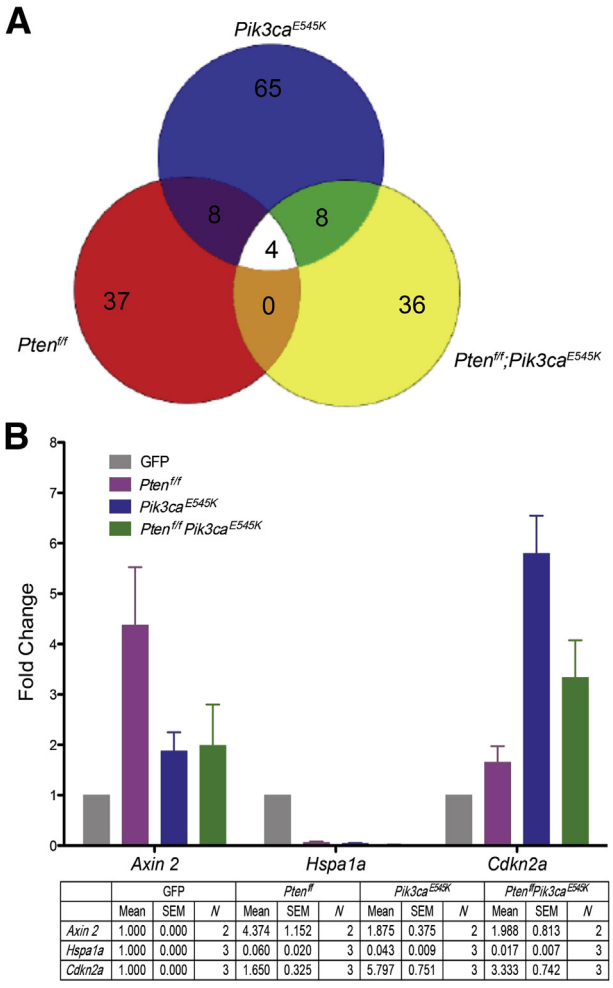

	GFP			*Pten*$^{f/f}$			*Pik3ca*^{E545K}			*Pten*$^{f/f}$*Pik3ca*^{E545K}		
	Mean	SEM	*N*	Mean	SEM	*N*	Mean	SEM	*N*	Mean	SEM	*N*
Axin 2	1.000	0.000	2	4.374	1.152	2	1.875	0.375	2	1.988	0.813	2
Hspa1a	1.000	0.000	3	0.060	0.020	3	0.043	0.009	3	0.017	0.007	3
Cdkn2a	1.000	0.000	3	1.650	0.325	3	5.797	0.751	3	3.333	0.742	3

Figure 4 RNA sequencing analysis. **A:** Venn diagram depicting the differentially expressed genes (DEGs) common and/or unique to *Pten*$^{f/f}$, *Pik3ca*^{E545K}, and *Pten*$^{f/f}$;*Pik3ca*^{E545K}. **B:** Real-time quantitative PCR analysis to validate expression of DEGs identified by RNA sequencing. Graph depicts fold change in expression of *Axin2*, *Hspa1a*, and *Cdkn2a* in *Pten*$^{f/f}$, *Pik3ca*^{E545K}, and *Pten*$^{f/f}$;*Pik3ca*^{E545K} cells as compared to green fluorescent protein (GFP)–treated cells. Means ± SEM are summarized. *N* = number of independent experiments performed for each gene.

described above and provides evidence that nuclear localization of FOXO1 is dependent on PTEN. In all of the cell lines, p-FOXO1 was detected maximally in the cytoplasmic compartment. The Hec1A cell lines (parent and clone) have a G1049R mutation in PIK3CA yet fail to activate AKT (Hec1A WT) in the absence of PTEN deletion (Hec1A clone).

Pten and *Pik3ca* Regulate Nonoverlapping Gene Sets

To delineate downstream changes in gene expression due to deletion of *Pten*, activation of *Pik3ca*, or both, we performed RNA sequencing analysis with RNA extracted from adeno-Cre–treated primary epithelial cell cultures prepared from *Pten*$^{f/f}$, *Pik3ca*^{E545K}, and *Pten*$^{f/f}$;*Pik3ca*^{E545K} mice. Deletion of *Pten* and expression of *Pik3ca*^{E545K} allele were confirmed at the RNA level by qPCR analysis (Supplemental Figure S2) and were submitted for RNA sequencing analysis.

A pairwise analysis was performed to individually compare control (GFP) with *Pten*$^{f/f}$, *Pik3ca*^{E545K}, and *Pten*$^{f/f}$;*Pik3ca*^{E545K} cells by setting a *P* cutoff at 0.05 and threefold differential expression. Only four genes were altered in all three conditions (Figure 4A). There was also minimal overlap between *Pten*$^{f/f}$ versus *Pik3ca*^{E545K} and *Pik3ca*^{E545K} versus *Pten*$^{f/f}$;*Pik3ca*^{E545K} cells. Most of the DEGs were unique to each condition (Supplemental Tables S3–S5). This finding suggests that deletion of *Pten* and activation of *Pik3ca* regulate distinct, nonoverlapping genes. For validation, we chose genes from the following groups: i) genes regulated in all of the groups (*Hspa1a*), ii) genes regulated in *Pik3ca*^{E545K} and *Pten*$^{f/f}$;*Pik3ca*^{E545K} cells (*Cdkn2a*), and iii) genes regulated maximally in *Pten*$^{f/f}$ cells (*Axin 2*). Validation was performed on cDNA from total RNA extracted from three independent cell preparations. Regulation of the three genes was similar to that observed by RNA sequencing (Figure 4B).

Discussion

Although *PTEN* and *PIK3CA* mutations occur at high frequencies in endometrial carcinoma, their respective roles in the neoplastic process remain unclear. We have been specifically interested in defining the consequences of these genetic alterations in the development of endometrial carcinoma. With the use of genetic mouse models reported herein, along with human tissue samples and cell lines, we have begun to dissect the impact of these two common genetic alterations on endometrial carcinogenesis.

We have shown that mouse strains with conditional deletion of *Pten*, as has been previously shown,[13,20] predictably develop endometrial hyperplasia that can progress to carcinoma. In contrast, the isolated activation of *Pik3ca* in the endometrial epithelium does not cause any phenotypic light microscopic changes. However, the activation of *Pik3ca* in the presence of *Pten* loss not only accelerates the progression to carcinoma, but leads to more extensive disease with extension into the ovaries. Interestingly, *Pik3ca* activation does not lead to the development of more extensive hyperplasia or carcinoma in the setting of *Pten* haploinsufficiency, and the frequency of CAH in *Pten*-haploinsufficient mice with or without *Pik3ca* activation was similar to germline *Pten*$^{+/-}$ mice[9] of the same age. This suggests that the rate-limiting step in the development of hyperplasia is the biallelic loss of Pten in the epithelium. The current findings corroborate the mutational analyses of primary human tumors and provide definitive evidence for a role of *Pten* in the development of hyperplasia, with *Pik3ca* driving the transition to invasion in the endometrial epithelium.

We present evidence from primary mouse cultures, as well as human cancer cell lines, that the extent of Akt phosphorylation differs between loss of *Pten* and activation of *Pik3ca*. Exon 9 and 20 mutations in p110α are hotspots common across all cancer types,[21,22] and these mutations

are equally effective in phosphorylating AKT in breast[23] and colorectal cancer[24] cell lines as well as primary urothelial cells.[25] However, in NIH3T3 cells, the kinase domain H1047R mutation was severalfold more potent than the helical domain E545K mutation at phosphorylating Akt, suggesting that the extent of pathway activation by these mutations (as seen by Akt phosphorylation) is cell context dependent.[25] In our studies, the E545K mutation resulted in a much less robust activation of Akt when compared to *Pten* in primary mouse endometrial epithelial cells. In human endometrial cancer cell lines as well, phosphorylated AKT was detected only in the cell lines with *PTEN* mutations (Figure 3E and Supplemental Table S2), despite the presence of a G1049R mutation in PIK3CA, as has been demonstrated previously.[26] In endometrial epithelial cells, therefore, both helical or kinase domain mutations were unable to overcome the inhibitory effects of PTEN, which likely explains, at least in part, the lack of phenotype in mice expressing only the activated *Pik3ca* allele. To our knowledge, this is the first report to provide mechanistic insights into the respective roles of *Pten* and *Pik3ca* in the endometrial epithelium *in vivo*. Recently, studies using mouse models of prostate and breast cancer highlighted the importance of p110β over p110α isoform, particularly in the context of *PTEN* deficiency.[27,28] It has also been suggested that the PI3K isoform dependence is affected by mutations in other genes.[29] However, p110β inhibition alone in endometrial cancer cell lines was ineffective at inducing apoptosis, irrespective of the *PTEN* status.[26]

FoxO1, a tumor-suppressor protein, is a well-characterized downstream target of Akt. Nuclear FoxO1 is a transcription factor activating expression of cell cycle inhibitors like p27 and p21, while repressing cyclins D1 and D2.[30] Activated Akt (as a result of Pten loss) phosphorylates FoxO1, leading to nuclear export, inhibiting its transcriptional activity and thus promoting cell proliferation and blocking apoptosis.[30] FOXO1 in humans and mice has been demonstrated to play a role in decidualization of stromal cells in the endometrium,[31–33] and its expression in the endometrial epithelium varies with the stage of the menstrual/estrus cycle.[34] Although UEC cases have been shown to express reduced FOXO1 as compared to the normal cycling endometrium,[19,35] there is a lack of evidence suggesting a direct link between *PTEN* mutation/inactivation and reduced expression. In our mouse models with CAH and UEC, FoxO1 expression was strikingly absent in the nucleus as compared to the normal epithelium, in agreement with the human data. As mentioned previously in *Results*, a TMA consisting of primary human tumors also showed lack of nuclear FOXO1 in 72% of cases. However, because activation of *Pik3ca* alone in the mouse uterus did not lead to endometrial disease, we were unable to dissect out the role of *Pten* and *Pik3ca* in regulating FoxO1 using mouse models. The human endometrial cancer cell lines proved ideal to investigate the link between FOXO1 and PTEN. Nuclear localization of FOXO1 correlated with presence of wild-type *PTEN*, irrespective of *PIK3CA* status in endometrial cancer cell lines. This was particularly evident in Hec1A WT and Hec1A clone 16 cells, which harbor a mutation in *PIK3CA* but differ from each other only with respect to the lack of *PTEN* in clone 16. Furthermore, KLE and RL95 (wild-type and mutant for *PTEN*, respectively) also exhibited similar localization of FOXO1. These observations provide evidence for a direct link between PTEN and FOXO1 in UEC. The lack of FOXO1 expression in most human UEC cases and its loss in hyperplasia and carcinoma in the mouse model suggest a central role for this transcription factor in the pathogenesis of endometrial carcinoma. Interestingly, FOXO1 expression was upregulated as a result of progestin treatment of immortalized and transformed endometrial epithelial cells[19,35,36] and is thought to mediate the progestin inhibition of epithelial proliferation. Regulating FOXO1 expression may be central to the mechanism by which *PTEN* promotes endometrial hyperplasia, most likely by inhibiting cell death rather than increasing proliferation. This is consistent with previous studies from our laboratory showing that CAH and UEC arising in the mouse model have lower proliferative indices than proliferative endometrium.[14] miRNA-mediated repression has also been implicated in the regulation of FOXO1 levels in the endometrial epithelium,[37,38] but its relationship to PTEN is currently unknown.

In addition to being less potent than Pten in activating Akt, Pik3ca also regulates transcription of a distinct set of genes *in vitro*, as demonstrated by RNA sequencing analysis of adeno-Cre–treated primary endometrial epithelial cell cultures. Furthermore, combined *Pten* deletion and *Pik3ca* activation altered expression of an entirely different set of genes as compared to *Pten* deletion or *Pik3ca* activation alone. Along with their roles as key players in the PI3K/AKT/PTEN pathway, *Pten* and *Pik3ca* may also individually participate in other cellular processes in the endometrial epithelium, providing a possible explanation for the frequent co-occurrence of mutations in primary human tumors.[11,39] Although these cell culture experiments are short-term and they may not recapitulate the complex genetic alterations observed in human cancers, they provide unique insights into immediate downstream effects of *Pten* deletion and/or *Pik3ca* activation. RNA sequencing on cells isolated from the lesions arising in different genotypes might more closely reflect the situation in human carcinogenesis.

In summary, the data presented herein provide unique insights into the respective roles of *PTEN* and *PIK3CA* in endometrial carcinoma. The PI3K/AKT pathway can be activated by many signals like estrogen or growth factors, secreted in a cyclic fashion in the endometrial epithelium, inducing proliferation and differentiation. The results presented above strongly support *PTEN* as the prominent suppressor of growth signals and show that the loss of *PTEN* removes the inhibition leading to hyperplasia and that *PIK3CA* mutations promote a transition to carcinoma. The mechanism underlying this transition may be related to further activation of AKT and likely regulation of other nonoverlapping downstream molecules. Currently, we are

pursuing the identification and characterization of molecules and pathways critical to the development of carcinoma.

Acknowledgment

Mice expressing Cre under the *Wnt7a* promoter (*Wnt7a-Cre*$^{+/-}$) were obtained from Dr. Kenneth S. Korach (National Institute of Environmental Health Science, Research Triangle Park, NC).

Supplemental Data

Supplemental material for this article can be found at *http://dx.doi.org/10.1016/j.ajpath.2014.12.019*.

References

1. Di Cristofano A, Ellenson LH: Endometrial carcinoma. Annu Rev Pathol 2007, 2:57−85
2. Tashiro H, Blazes MS, Wu R, Cho KR, Bose S, Wang SI, Li J, Parsons R, Ellenson LH: Mutations in PTEN are frequent in endometrial carcinoma but rare in other common gynecological malignancies. Cancer Res 1997, 57:3935−3940
3. Salvesen HB, Stefansson I, Kretzschmar EI, Gruber P, MacDonald ND, Ryan A, Jacobs IJ, Akslen LA, Das S: Significance of PTEN alterations in endometrial carcinoma: a population-based study of mutations, promoter methylation and PTEN protein expression. Int J Oncol 2004, 25: 1615−1623
4. Risinger JI, Hayes K, Maxwell GL, Carney ME, Dodge RK, Barrett JC, Berchuck A: PTEN mutation in endometrial cancers is associated with favorable clinical and pathologic characteristics. Clin Cancer Res 1998, 4:3005−3010
5. Cantley LC: The phosphoinositide 3-kinase pathway. Science 2002, 296:1655−1657
6. Song MS, Salmena L, Pandolfi PP: The functions and regulation of the PTEN tumour suppressor. Nat Rev Mol Cell Biol 2012, 13:283−296
7. Risinger JI, Hayes AK, Berchuck A, Barrett JC: PTEN/MMAC1 mutations in endometrial cancers. Cancer Res 1997, 57:4736−4738
8. Kanamori Y, Kigawa J, Itamochi H, Shimada M, Takahashi M, Kamazawa S, Sato S, Akeshima R, Terakawa N: Correlation between loss of PTEN expression and Akt phosphorylation in endometrial carcinoma. Clin Cancer Res 2001, 7:892−895
9. Wang H, Douglas W, Lia M, Edelmann W, Kucherlapati R, Podsypanina K, Parsons R, Ellenson LH: DNA mismatch repair deficiency accelerates endometrial tumorigenesis in Pten heterozygous mice. Am J Pathol 2002, 160:1481−1486
10. Wang H, Joshi A, Iaconis L, Solomon GJ, Xiang Z, Verhage HG, Douglas W, Ronnett BM, Ellenson LH: Oviduct-specific glycoprotein is a molecular marker for invasion in endometrial tumorigenesis identified using a relevant mouse model. Int J Cancer 2009, 124: 1349−1357
11. Hayes MP, Wang H, Espinal-Witter R, Douglas W, Solomon GJ, Baker SJ, Ellenson LH: PIK3CA and PTEN mutations in uterine endometrioid carcinoma and complex atypical hyperplasia. Clin Cancer Res 2006, 12:5932−5935
12. Hayes MP, Ellenson LH: Molecular alterations in uterine serous carcinoma. Gynecol Oncol 2010, 116:286−289
13. Joshi A, Ellenson LH: Adenovirus mediated homozygous endometrial epithelial Pten deletion results in aggressive endometrial carcinoma. Exp Cell Res 2011, 317:1580−1589
14. Joshi A, Wang H, Jiang G, Douglas W, Chan JS, Korach KS, Ellenson LH: Endometrial tumorigenesis in Pten(+/-) mice is independent of coexistence of estrogen and estrogen receptor alpha. Am J Pathol 2012, 180:2536−2547
15. Winuthayanon W, Hewitt SC, Orvis GD, Behringer RR, Korach KS: Uterine epithelial estrogen receptor alpha is dispensable for proliferation but essential for complete biological and biochemical responses. Proc Natl Acad Sci U S A 2010, 107:19272−19277
16. Wild PJ, Ikenberg K, Fuchs TJ, Rechsteiner M, Georgiev S, Fankhauser N, Noske A, Roessle M, Caduff R, Dellas A, Fink D, Moch H, Krek W, Frew IJ: p53 Suppresses type II endometrial carcinomas in mice and governs endometrial tumour aggressiveness in humans. EMBO Mol Med 2012, 4:808−824
17. Frew IJ, Minola A, Georgiev S, Hitz M, Moch H, Richard S, Vortmeyer AO, Krek W: Combined VHLH and PTEN mutation causes genital tract cystadenoma and squamous metaplasia. Mol Cell Biol 2008, 28:4536−4548
18. Shao X, Somlo S, Igarashi P: Epithelial-specific Cre/lox recombination in the developing kidney and genitourinary tract. J Am Soc Nephrol 2002, 13:1837−1846
19. Ward EC, Hoekstra AV, Blok LJ, Hanifi-Moghaddam P, Lurain JR, Singh DK, Buttin BM, Schink JC, Kim JJ: The regulation and function of the forkhead transcription factor, Forkhead box O1, is dependent on the progesterone receptor in endometrial carcinoma. Endocrinology 2008, 149:1942−1950
20. Daikoku T, Hirota Y, Tranguch S, Joshi AR, DeMayo FJ, Lydon JP, Ellenson LH, Dey SK: Conditional loss of uterine Pten unfailingly and rapidly induces endometrial cancer in mice. Cancer Res 2008, 68: 5619−5627
21. Campbell IG, Russell SE, Choong DY, Montgomery KG, Ciavarella ML, Hooi CS, Cristiano BE, Pearson RB, Phillips WA: Mutation of the PIK3CA gene in ovarian and breast cancer. Cancer Res 2004, 64:7678−7681
22. Samuels Y, Wang Z, Bardelli A, Silliman N, Ptak J, Szabo S, Yan H, Gazdar A, Powell SM, Riggins GJ, Willson JK, Markowitz S, Kinzler KW, Vogelstein B, Velculescu VE: High frequency of mutations of the PIK3CA gene in human cancers. Science 2004, 304:554
23. Zhao JJ, Liu Z, Wang L, Shin E, Loda MF, Roberts TM: The oncogenic properties of mutant p110alpha and p110beta phosphatidylinositol 3-kinases in human mammary epithelial cells. Proc Natl Acad Sci U S A 2005, 102:18443−18448
24. Samuels Y, Diaz LA Jr, Schmidt-Kittler O, Cummins JM, Delong L, Cheong I, Rago C, Huso DL, Lengauer C, Kinzler KW, Vogelstein B, Velculescu VE: Mutant PIK3CA promotes cell growth and invasion of human cancer cells. Cancer Cell 2005, 7:561−573
25. Ross RL, Askham JM, Knowles MA: PIK3CA mutation spectrum in urothelial carcinoma reflects cell context-dependent signaling and phenotypic outputs. Oncogene 2013, 32:768−776
26. Weigelt B, Warne PH, Lambros MB, Reis-Filho JS, Downward J: PI3K pathway dependencies in endometrioid endometrial cancer cell lines. Clin Cancer Res 2013, 19:3533−3544
27. Wee S, Wiederschain D, Maira SM, Loo A, Miller C, deBeaumont R, Stegmeier F, Yao YM, Lengauer C: PTEN-deficient cancers depend on PIK3CB. Proc Natl Acad Sci U S A 2008, 105:13057−13062
28. Jia S, Liu Z, Zhang S, Liu P, Zhang L, Lee SH, Zhang J, Signoretti S, Loda M, Roberts TM, Zhao JJ: Essential roles of PI(3)K-p110beta in cell growth, metabolism and tumorigenesis. Nature 2008, 454: 776−779
29. Schmit F, Utermark T, Zhang S, Wang Q, Von T, Roberts TM, Zhao JJ: PI3K isoform dependence of PTEN-deficient tumors can be altered by the genetic context. Proc Natl Acad Sci U S A 2014, 111: 6395−6400
30. Lam EW, Brosens JJ, Gomes AR, Koo CY: Forkhead box proteins: tuning forks for transcriptional harmony. Nat Rev Cancer 2013, 13: 482−495
31. Buzzio OL, Lu Z, Miller CD, Unterman TG, Kim JJ: FOXO1A differentially regulates genes of decidualization. Endocrinology 2006, 147:3870−3876
32. Kajihara T, Jones M, Fusi L, Takano M, Feroze-Zaidi F, Pirianov G, Mehmet H, Ishihara O, Higham JM, Lam EW, Brosens JJ: Differential

expression of FOXO1 and FOXO3a confers resistance to oxidative cell death upon endometrial decidualization. Mol Endocrinol 2006, 20: 2444–2455

33. Labied S, Kajihara T, Madureira PA, Fusi L, Jones MC, Higham JM, Varshochi R, Francis JM, Zoumpoulidou G, Essafi A, Fernandez de Mattos S, Lam EW, Brosens JJ: Progestins regulate the expression and activity of the forkhead transcription factor FOXO1 in differentiating human endometrium. Mol Endocrinol 2006, 20:35–44
34. Fan W, Li SW, Li WH, Wang Y, Gong Y, Ma QH, Luo S: FOXO1 expression and regulation in endometrial tissue during the menstrual cycle and in early pregnancy decidua. Gynecol Obstet Invest 2012, 74:56–63
35. Goto T, Takano M, Albergaria A, Briese J, Pomeranz KM, Cloke B, Fusi L, Feroze-Zaidi F, Maywald N, Sajin M, Dina RE, Ishihara O, Takeda S, Lam EW, Bamberger AM, Ghaem-Maghami S, Brosens JJ: Mechanism and functional consequences of loss of FOXO1 expression in endometrioid endometrial cancer cells. Oncogene 2008, 27:9–19
36. Kyo S, Sakaguchi J, Kiyono T, Shimizu Y, Maida Y, Mizumoto Y, Mori N, Nakamura M, Takakura M, Miyake K, Sakamoto M, Inoue M: Forkhead transcription factor FOXO1 is a direct target of progestin to inhibit endometrial epithelial cell growth. Clin Cancer Res 2011, 17: 525–537
37. Myatt SS, Wang J, Monteiro LJ, Christian M, Ho KK, Fusi L, Dina RE, Brosens JJ, Ghaem-Maghami S, Lam EW: Definition of microRNAs that repress expression of the tumor suppressor gene FOXO1 in endometrial cancer. Cancer Res 2010, 70:367–377
38. Mozos A, Catasus L, D'Angelo E, Serrano E, Espinosa I, Ferrer I, Pons C, Prat J: The FOXO1-miR27 tandem regulates myometrial invasion in endometrioid endometrial adenocarcinoma. Hum Pathol 2014, 45:942–951
39. Oda K, Stokoe D, Taketani Y, McCormick F: High frequency of coexistent mutations of PIK3CA and PTEN genes in endometrial carcinoma. Cancer Res 2005, 65:10669–10673